LASER & PHOTONICS REVIEWS
www.lpr-journal.org

How Do the Purcell Factor, the *Q*-Factor, and the Beta Factor Affect the Laser Threshold?

Jacob B. Khurgin and Mikhail A. Noginov*

Dedicated to the memory of Professor Mark I. Stockman (1947–2020), a pioneer in the field of nano optics and co-inventor of the spaser, among many other breakthrough discoveries. Mark's talent, devotion to science, zest for life, and indomitable spirit have inspired many, including us, and will continue to inspire new generations of scientists.

As lasers get more and more miniaturized and their dimensions become comparable to the wavelength, two interconnected phenomena take place: the fraction of spontaneous radiation going into a specific laser mode (β-factor) increases and can ultimately reach unity, while the radiative lifetime gets shortened by the Purcell factor F_p. Often it is assumed that an increase of these two factors, along with the quality factor (*Q*-factor), almost invariably causes reduction of the lasing threshold. This assumption is tested on various photonic and plasmonic lasers, demonstrating that, while there is obvious correlation between the aforementioned factors and the laser threshold, the dependence is far from being straightforward and omnipresent. Depending on specific laser material and geometry, the threshold can decrease, increase, or stay unchanged when β-factor, *Q*-factor, and F_p increase. For the most part, the reduction of threshold is achieved simply by reducing the laser volume and this volume reduction can concurrently cause the increase in β-factor and/or Purcell factor, but it would be imprudent to say that the increase in either of these factors is the cause of the threshold reduction.

1. Introduction

Lasers have become omnipresent in the society, being indispensable in telecommunications, manufacturing, health care, defense, and many other fields of human endeavor.[1–3] The development of lasers is moving toward many diverse objectives, such as increasing power and/or modulation speed, improving tunability, reducing the linewidth, and many others. Among them, one goal stands out, the one of miniaturization of lasers and integration them with other optical and electronic devices. Recent years have seen rapid progress along the path of laser miniaturization. Some of the smallest vertical cavity surface emitting lasers with dimensions of few micrometers,[4] have already entered the mainstream and are widely used in local area networks and data centers.[5] Meanwhile the research has moved on to even smaller dimensions, approaching and surpassing the diffraction limit and introducing such new terms as "nanolaser"[6–8] and "spaser"[9–11] into our vocabulary. A wide variety of nanolasers have been proposed, with large fraction of them fabricated and investigated. The lasers differed in terms of active media—III–V[8,12–14] and II–VI semiconductors,[11,15,16] 2D materials,[17] organic dye molecules,[9,18] rare earth ions,[19] in terms of pumping—optical or electrical, and, most significant, in terms of cavity design. Since diffraction losses make conventional cavity designs such as Fabry–Perot cavity, spherical mirror resonators, and others impractical for nanolasers, different designs have been suggested and tried, such as micro ring resonators,[20,21] whispering gallery mode (WGM) resonators,[22] photonic crystal resonators,[7,8,17,23] and so on. However, these dielectric-based resonators, to which we shall refer to as "photonic," are not capable of confining the light into subwavelength volume, hence various designs involving metal and hybrid metal-dielectric cavities have been proposed and tested. In metals the exited modes are so-called localized surface plasmon (LSP) and surface plasmon polariton (SPP), comprised by a photon and a collective oscillation of electrons, plasmon. The effective wavelength of SPP is smaller than free space wavelength; therefore, subwavelength confinement of electric field is attainable, albeit at a cost of large loss. Therefore, the metal-containing laser cavities are often referred to as "plasmonic," even though more often than not this designation is not technically correct as for most metal clad lasers a very small fraction of energy resides in the metal.[24,25] Only when the laser becomes subwavelength in all three dimensions, significant fraction of energy resides in collective oscillations of free carriers.[26,27] (such laser is also called "spaser"[10]). Despite that, we shall stick with the moniker "plasmonic" for all metal containing cavities

Prof. J. B. Khurgin
Department of Electrical and Computer Engineering, Johns Hopkins University Baltimore
Baltimore, MD 21218, USA
E-mail: jakek@jhu.edu
Prof. M. A. Noginov
Center for Materials Research
Norfolk State University
Norfolk, VA 23504, USA

The ORCID identification number(s) for the author(s) of this article can be found under https://doi.org/10.1002/lpor.202000250

DOI: 10.1002/lpor.202000250

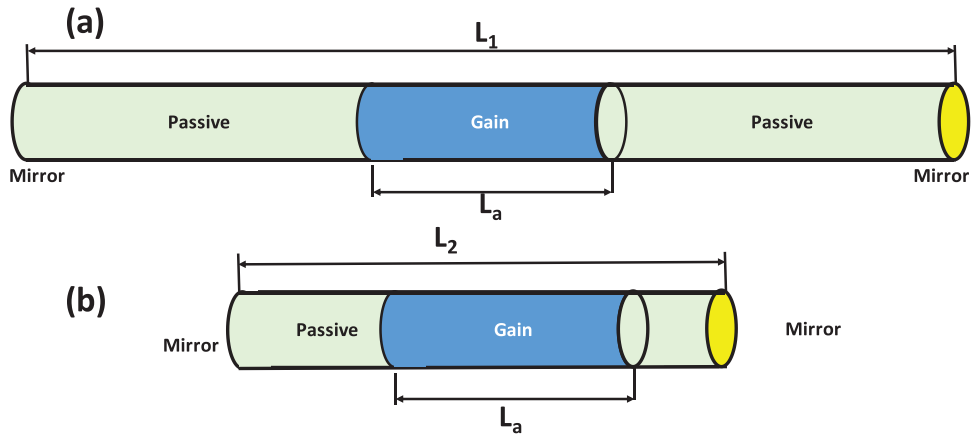

Figure 1. Two lasers with a) longer and b) shorter cavity lengths have different β, Q and F_P but the same threshold.

such as metal–insulator–metal (MIM) waveguides,[12,28] Fabry–Perot cavities,[29] coaxial cavities,[13] metal clad dielectric, metal nanoparticles immersed into the laser gain medium,[30,31] and many others that have been investigated. There are still significant obstacles that prevent metal-based nanolasers from becoming practical, mostly due to inherently high loss in metal makes the lasing threshold high. But the steady if slow progress is being made in both photonic and plasmonic nanolasers (spasers) as can be learned from a number of excellent review publications.[6,32–39]

This work is intended as a pedagogical one and not as review article; hence, it is impossible to mention each and every contribution made in the field of nanolasers, and, besides this point, a number of aforementioned reviews on this topic is available. Therefore, we shall now turn our attention to the main subject of this study, which is what exactly is the influence of spontaneous emission factor β, Q-factor, and the Purcell factor F_P on the laser characteristics, most notably, the lasing threshold? The literature is full of mentions that somehow increasing either one of β,[40,41] Q,[42,43] and F_P,[44–48] or preferentially, all of them is bound to boost the laser performance. This claim has become unquestionable for many researchers (with some notable exceptions,[14,27,49]) even though, to the best of our knowledge, no rigorous proof of it had been given. In fact, both β and F_P are related to spontaneous emission, and in a laser, spontaneous emission plays less than constructive role. So, it is not obvious how enhancing spontaneous emission should make a laser better. A simple illustration of the fact that relation between β, Q, and the lasing threshold is not straightforward is provided by **Figure 1**, where the laser gain medium of length L_a is inserted in Fabry–Perot cavity of length L. If we now compare two cavities with the same active medium length, but with different cavity lengths, $L_2 < L_1$, the spontaneous emission factor β decreases with length, $\beta_1 < \beta_2$, while the Q-factor increases with length, $Q_1 > Q_2$. Furthermore, if the gain bandwidth is sufficiently narrow, the Purcell factor decreases, $F_{P1} < F_{P2}$. However, the laser threshold, obviously, does not change (assuming that diffraction loss is small). Therefore, we believe that is important to re-examine rigorously what role, if any, β, Q, and F_P play in the nanolasers. Once again, we re-iterate that the objective of this work is not to lay any claim of novelty to something that is implicitly well understood within laser engineering community, where discourse is always done in terms of

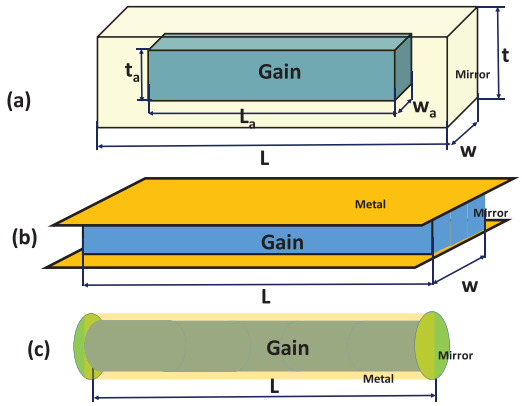

Figure 2. Simplified geometry of three different cavity types. a) 3D photonic cavity, b) 2D plasmonic waveguide cavity, c) 1D plasmonic nanowire cavity.

well-established parameters of volumes and confinement factors, with neither β nor F_P mentioned at all. But the field of nanolasers has justifiably attracted a large number of entrants from other branches of physics and technology, where that knowledge has not yet set in. Consequently, there is a certain degree of over emphasizing the positive role of β, Q, and F_P, while omitting the deleterious role. This can lead to serious consequences (as shown in a simple example of Figure 1), thus we believe that a rigorous and pedagogical discussion, as attempted in this work, should play constructive role.

2. Photonic and Plasmonic Cavities

We consider three different types of cavities—one photonic and two plasmonic. A photonic cavity is shown in **Figure 2**a, and is defined by the mode thickness t, width w, and length L. When $L >> t, w$, the laser cavity is conventional, or edge-emitting, and if $L < t, w$, one is dealing with a surface emitting laser. The excited active medium providing laser gain sometimes does not fill the entire mode volume and is characterized by the active medium dimensions, t_a, w_a, and L_a. Note that in this work we define active volume as the volume that is being pumped

and not just the volume of let us say entire laser crystal. A (transverse) $\Gamma = w_a t_a / wt$ confinement factor can be introduced. It is expedient to normalize all the dimensions to wavelength in medium as $t' = 2nt/\lambda$ and so on. The mode volume can be defined by a Fabry–Perot-like external cavity or by a waveguide with thickness and width comparable to a half-wavelength in the material, but, for the purpose of our analysis, it will not make a difference. What is important is that in the photonic cavity, whether it is an external resonator with Gaussian mode or a dielectric waveguide, the spontaneous radiation can always be emitted into a 3D space, defined by the 3D density of states[50]

$$\rho_{3D} = \frac{1}{\pi^2}\frac{n^2 n_g}{c^3}\omega^2 = \frac{8\pi n^3 n_g'}{\lambda^3}\frac{1}{\omega} \tag{1}$$

where n is refractive index, $n_g = cdk/d\omega$ is a group index, and $n_g' = n_g/n$ is the normalized value of group index. If we now look at the plasmonic waveguide of Figure 2b with the gap thickness less than $\lambda/2n$, the active medium can only emit into the 2D density of states

$$\rho_{2D} = \frac{1}{\pi}\frac{n_e \omega n_g}{c^2} = \frac{4\pi n^2}{\lambda^2}\frac{1}{\omega} n_e' n_g' \tag{2}$$

where n_e and n_g are the effective index and group index of the waveguide, respectively, and $n_e' = n_e/n$ and $n_g' = n_g/n$ are the normalized values.

Finally, we consider a 1D plasmonic nanowire (Figure 2c) with subwavelength cross section (probably not a simple structure to realize), where 1D density of states is

$$\rho_{1D} = \frac{2}{\pi}\frac{n_g}{c} = \frac{4nn_g'}{\lambda\omega} \tag{3}$$

3. Beta-Factor

We assume that if the spontaneous emission is characterized by the effective bandwidth $\Delta\omega$, then the total number of modes in the photonic cavity is

$$\beta_{3D,0}^{-1} = V\rho_{3D}\Delta\omega = \pi V'\frac{\Delta\omega}{\omega} n_g' \tag{4}$$

where the normalized volume is $V' = t'w'L'$ and normalized dimensions are $w' = 2nw/\lambda$, $t' = 2nt/\lambda$ and $L' = 2nL/\lambda$. For the plasmonic waveguide

$$\beta_{2D,0}^{-1} = wL\rho_{2D}\Delta\omega = \pi w' L'\frac{\Delta\omega}{\omega} n_e' n_g' \tag{5}$$

and for the nanowire

$$\beta_{1D,0}^{-1} = L\rho_{2D}\Delta\omega = 2L'\frac{\Delta\omega}{\omega} n_g' \tag{6}$$

But, of course, one shall remember that the number of modes cannot be less than 1, so one can use the approximation

$$\beta_i^{-1} = \mathrm{Int}(\beta_{i,0}^{-1} + 1) \tag{7}$$

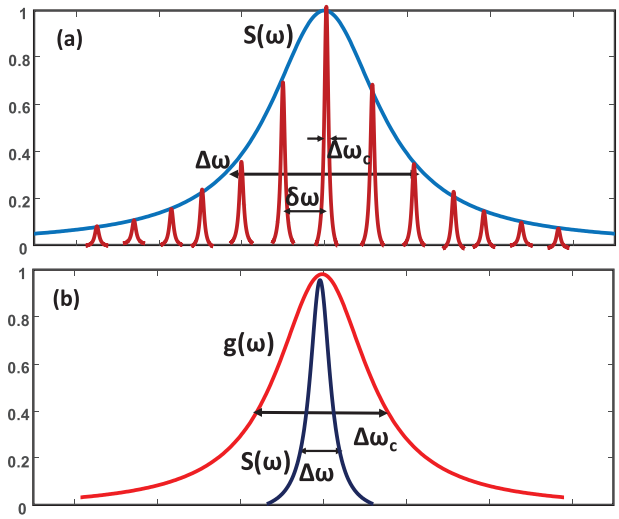

Figure 3. Spontaneous emission spectrum of the gain medium $S(\omega)$ with laser modes whose line-shape is $g(\omega)$. $\Delta\omega$ is the emission spectral width, $\delta\omega$ is the mode spacing, and $\Delta\omega_c$ is the mode linewidth. a) Multimode laser with broad gain and narrow cavity linewidth. b) Single mode (typically plasmonic) laser with very broad cavity linewidth.

where index i refers to the dimensionality of the cavity. This estimate creates the curve that is not really smooth because the emission power spectrum $S(\omega)$ was assumed to be a "rectangular shape" function of width $\Delta\omega$. In reality, the distribution is smooth, $S(\omega)$ has a maximum $S_{max} = 1$, and the spectral width is $\Delta\omega = \int S(\omega)d\omega$. Note that $\Delta\omega$ is not exactly an FWHM width of the spontaneous emission $\omega_{1/2}$. If we assume Lorentzian lineshape as in **Figure 3**a, $\Delta\omega = \frac{\pi}{2}\omega_{1/2}$, and for Gaussian lineshape $\Delta\omega = \frac{1}{2}\sqrt{\frac{\pi}{\ln 2}}\omega_{1/2}$. The correct expression for the β-factor is then

$$\beta_i^{-1} = \sum_m \int S(\omega)g(\omega - \omega_m)d\omega \Big/ \int S(\omega)g(\omega - \omega_l)d\omega \tag{8}$$

where ω_m are the cavity modes frequencies, ω_l is the frequency of the lasing mode, and $g(\omega)$ is the normalized line shape of the cavity, typically approximated as a Lorentzian with FWHM $\Delta\omega_c$. In most practical lasers, other than ones using plasmonic nanoparticles, the cavity linewidth $\Delta\omega_c$ is much narrower than the linewidth of spontaneous emission $\Delta\omega$, hence, the cavity line shape can be approximated as $\delta(\omega - \omega_m)$. In the opposite limit, when $\Delta\omega_c > \Delta\omega$, shown in Figure 3b, obviously, $\beta = 1$; we shall consider that case separately. Furthermore, in most cases, the lasing mode is very close to the maximum of spontaneous emission so $S(\omega_l) \approx 1$ and

$$\beta_i \approx 1/\sum_m S(\omega - \omega_m) \tag{9}$$

Therefore, as the intermodal distance $\delta\omega \sim 1/\rho_{3D}V = \omega/\pi V'$ for the 3D photonic cavity (or $\delta\omega \sim 1/\rho_{2D}wL$ for the 2D plasmonic waveguide and $\delta\omega \sim 1/\rho_{1D}L$ for 1D plasmonic nanowire) gets increased, β increases to unity smoothly as shown in **Figure 4**a. In that figure the horizontal axis is in relative units, i.e., normalized volume is V', and we have introduced the quality factor of emitter

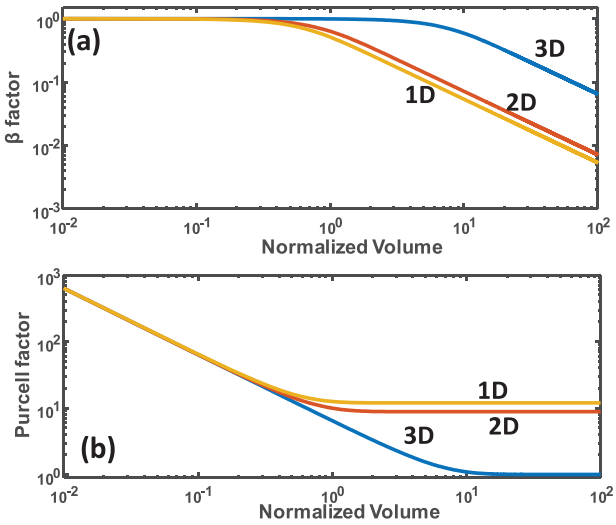

Figure 4. a) Spontaneous emission factor β and b) Purcell factor F_P as functions of normalized cavity volume V'.

$Q_{em} = \omega/\Delta\omega = 20$. In the estimate we assume that the 2D plasmonic waveguide thickness is $t = \lambda/10n(t' = 0.2)$, $n_e' = 1.2$, and that for the plasmonic nanowire the channel width is $w = \lambda/5n$. With these realistic assumptions the three curves in Figure 4a nearly overlap (at small normalized volumes) just as expected. It is easy to see that for large cavities the modes are closely spaced and the expressions (4)–(6) and (9) yield identical results, $\beta \approx \beta_0$ But for very small cavities, $\beta_{0,i}^{-1} \to 0$, which is obviously nonphysical, while from (9), $\beta_i^{-1} \to 1$, hence, one must use (9).

Note that for the same $V' > 1$ volume 2D and 1D cavities have lower β factors than 3D cavity. That is easy to understand—since one (two) transverse dimensions in 2D (1D) are subwavelength ($w', t' < 1$) a single transverse mode is still supported no matter how small are those dimensions. Hence to have the same volume as 3D cavity whose transverse dimensions are not subwavelength ($w', t' > 1$) the lower-dimensionality cavities must be longer which increases the number of longitudinal modes hence reducing β. For the lasers that are subwavelength in all three dimensions the distinctions between 1D, 2D, and 3D cavities of course disappear.

4. Purcell Factor

The Purcell factor[51] is defined as $F_P = \tau_{rad}^{-1}/\tau_{rad,0}^{-1}$, i.e., the ratio between the radiative decay rate of the emitter placed in a cavity $\tau_{rad}^{-1} = \sum_m \tau_{rad,m}^{-1}$ (where $\tau_{rad,m}^{-1}$ is a decay rate into a single mode) and the decay rate of the same emitter in an unconstrained dielectric space $\tau_{rad,0}^{-1}$. For the emitter with frequency ω, the rate of emission into the m^{th} mode can be found as $\tau_{rad,m}^{-1} = \frac{2\pi}{\hbar} M^2 g(\omega - \omega_m)/V$, where M is the matrix element of the interaction between the emitter and photon, hence

$$F_{P,3D} = \frac{\sum_m \int S(\omega) g(\omega - \omega_m) d\omega}{V \int S(\omega) \rho_{3D}(\omega) d\omega}; \frac{\beta^{-1}}{V \rho_{3D} \Delta\omega} = \frac{\beta_{3D,0}}{\beta_i} \quad (10)$$

where $\beta_{3D,0}$ has been defined in (4). Therefore, for the photonic cavity, as long as $\beta_{3D} < 1$, $F_P \approx 1$ but once β_{3D} approaches unity, which occurs roughly when $\pi V' Q_{em} = 1$,as volume continues to decrease,

$$F_{P,3D} = \beta_{3D0} = Q_{em}/\pi V' \quad (11)$$

Similarly, for the 2D plasmonic waveguide cavity

$$F_{P,2D} \approx \frac{\beta_{1D}^{-1}}{\beta_{3D,0}^{-1}} = \frac{\beta_{2D}^{-1}}{\beta_{2D,0}^{-1}} \frac{n_e' n_g'}{t'} \quad (12)$$

Therefore, as long as $\beta_{2D} < 1, F_{P,2D} = n_e' n_g'/t'$, but once β_{2D} approaches unity, which occurs when $\pi w' L' n_e' n_g'/Q_{em} = 1$, the Purcell factor is determined only by the volume and bandwidth $F_{P2D} = Q_{em}/\pi V'$, which is the same result as (11) derived for 3D cavity.

Finally, for the 1D metal clad nanowire waveguide

$$F_{1D} \approx \frac{\beta_{1D}^{-1}}{\beta_{3D,0}^{-1}} = \frac{\beta_{1D}^{-1}}{\beta_{1D,0}^{-1}} \frac{2}{\pi} \frac{n_g'}{S'} \quad (13)$$

where $S' = t'w'$ is a normalized cross-section area of the waveguide. With this introduction of area, (13) can be used for any shape of the mode cross-section rather than only for the not very common rectangular one. For as long as $\beta_{nw} < 1$, Purcell factor remains $F_{P,1D} = \frac{2}{\pi} \frac{n_g'}{S'}$, and once β approaches unity, which occurs when $2L' n_g'/Q_{em} = 1$, and once again (11) $F_{P,nw} = Q_{em}/\pi V'$.

Therefore, for single mode cavities, Purcell factor is always determined only by the mode volume and the emission bandwidth. Note though that the fact that there is only a single mode inside the cavity, it does not mean that the cavity is subwavelength. Also, it is important to note that for large volume multimode photonic cavities, $t', w' > 1$ and Purcell factor (almost) does not exceed unity. However, for plasmonic waveguides and nanowires, the cross-section can be substantially subwavelength and, coupled with the large group index, the Purcell factor of up to 10 can be attained even in the cavities with more than a single mode. The fact that for 2D and 1D cavities Purcell factor can be larger than unity even if the volume is not subwavelength is not surprising since even when only one or two transverse dimensions are reduced and $t', w' < 1$ the vacuum field in each mode is increased compared to free space, which causes Purcell enhancement. Last but not least, note that the product of Purcell factor and β-factor in any structure (i.e., the relation between the radiative decay rate into a given mode τ_{rad}^{-1} and the radiative decay in the free space $\tau_{rad,0}^{-1}$) is always the same

$$\tau_{rad,m}^{-1}/\tau_{rad,0}^{-1} = F_P \beta = Q_{em}/\pi V' \quad (14)$$

Reduction of volume can only change either one of two factors: for larger cavities only β can be changed and only once $\beta \approx 1$, the Purcell factor increases. This fact can be clearly seen in Figure 4b where we have plotted Purcell factors for the same three cavity types as in Figure 4a.

Now, if the cavity linewidth $\Delta\omega_c$ significantly exceeds the gain emission bandwidth $\Delta\omega$, as shown in Figure 3b, the emission

spectrum in (10) can be approximated with a delta function and the Purcell factor[51] becomes

$$F_{\mathrm{p}} = \frac{g_{\max}(\omega)}{V\rho_{3\mathrm{D}}} \approx \frac{1/\Delta\omega}{V'\pi/\omega} = \frac{Q_{\mathrm{cav}}}{\pi V'} \tag{15}$$

which is the case of a lossy plasmonic medium. Overall, one can use effective quality factor, $Q^{-1} = Q_{\mathrm{em}}^{-1} + Q_{\mathrm{cav}}^{-1}$ to describe the general case.

5. Spontaneous and Stimulated Emission Rates

The relation between stimulated and spontaneous emission is well established and can be traced to the relation between the Einstein coefficients[3] or to the relation between the eigenvalues of the operators of photon creation and annihilation.[50] Nevertheless, the confusion exists due to the fact that stimulated emission is usually characterized by such parameters as gain or stimulated emission cross-section, which are not explicitly related to the spontaneous emission rate. Considering pedagogical objectives of this work, we explore these relations in this section.

Let us first write down the rate equation for number of photons in one mode n_{p}. We consider a two-level atom-like system, in which the ground state and the excited state are separated by energy $\hbar\omega$, with population of lower and upper levels equal to n_1 and n_2, respectively. For as long as the light–matter coupling is weak,[52] which is a regime in which most lasers operate, the rate equation is

$$\frac{\mathrm{d}n_{\mathrm{p}}}{\mathrm{d}t} = -b_{12}n_1n_{\mathrm{p}} + b_{21}n_2n_{\mathrm{p}} + \frac{n_2}{\tau_{\mathrm{rad,m}}} \tag{16}$$

where $1/\tau_{\mathrm{rad,m}}$ is the rate of radiative decay into a single mode and b_{12}, b_{21} are respectively the coefficients of absorption and stimulated emission into the same single mode. The latter coefficients are related to Einstein coefficients B as $B_{12} = b_{12}V/\hbar\omega$, where V is the mode volume. (Note that so-called polaritonic[53]lasers operating a strong coupling regime are not discussed in the present tutorial.) At equilibrium, the photon occupation is defined by the Bose–Einstein statistics, while the level populations are related as $n_1 = n_2\exp(\hbar\omega/kT)$), which amounts to

$$n_{\mathrm{p}} = \frac{n_2\tau_{\mathrm{rad}}^{-1}}{b_{12}n_1 - b_{21}n_2} = \frac{\tau_{\mathrm{rad,m}}^{-1}/b_{12}}{e^{\frac{\hbar\omega}{kT}} - b_{21}/b_{12}} \equiv \frac{1}{e^{\frac{\hbar\omega}{kT}} - 1} \tag{17}$$

Therefore, as, of course, should follow from the fully quantum description of photons using creation and annihilation operators[50]

$$b_{12} = b_{21} = \tau_{\mathrm{rad,m}}^{-1} = \tau_{\mathrm{rad},0}^{-1}Q_{\mathrm{em}}/\pi V' \tag{18}$$

The rates of spontaneous and stimulated emission per photon are equal to each other, as spontaneous decay can be simply understood in terms of stimulated decay caused by "the vacuum fluctuation photon." Therefore, any Purcell enhancement of spontaneous decay rate will always be accompanied by the commensurate enhancement of the stimulated decay rate. It is based on that enhancement of stimulated rate that many erroneous projections in the field of nanolasers have been made. Hence, it is important to note that while the rate of stimulated emission gets enhanced, the stimulated emission cross-section does not change as it is an intrinsic material parameter that does not get changed by the size or shape of the cavity.

As long as there are n_{p} photons in a given mode, the power of the radiation propagating along the x axis in one direction is $P = \hbar\omega n_{\mathrm{p}}c/2n_{\mathrm{g}}L$. The densities of excited and ground states atoms is N_2 and N_1 respectively. The rate of energy change in the small volume of active medium $\mathrm{d}V = t\cdot w\cdot \mathrm{d}z$ is then

$$\begin{aligned}\frac{\mathrm{d}U}{\mathrm{d}t} &= \hbar\omega\mathrm{d}V(N_2 - N_1)\frac{n_{\mathrm{p}}}{\tau_{\mathrm{rad,m}}}\\ &= \hbar\omega twL(N_2 - N_1)\times\frac{2n_{\mathrm{g}}LP}{\hbar\omega c}\frac{(\lambda/2n)^3}{\pi twL}\frac{\omega}{\Delta\omega}\frac{\mathrm{d}z}{\tau_{\mathrm{rad},0}}\\ &= 2Pn_{\mathrm{g}}'\frac{(N_2 - N_1)(\lambda/2n)^2}{\Delta\omega\tau_{\mathrm{rad},0}}\mathrm{d}z\end{aligned} \tag{19}$$

where (18) and then (14) have been used, and, since change of power going into one direction is $\mathrm{d}P/\mathrm{d}z = \frac{1}{2}\mathrm{d}U/\mathrm{d}t$, one obtains

$$\frac{\mathrm{d}P}{\mathrm{d}z} = Pn_{\mathrm{g}}'\frac{(N_2 - N_1)(\lambda/2n)^2}{\Delta\omega\tau_{\mathrm{rad},0}} = n_{\mathrm{g}}'\sigma_{21}(N_2 - N_1)P \tag{20}$$

Here, the stimulated emission cross-section $\sigma_{21} = \lambda^2/4n^2\Delta\omega\tau_{\mathrm{rad},0}$ is totally independent of any cavity characteristics, be that β, Q, or Purcell factor (as long as we limit our discussion to the weak light–matter interaction regime). One should note that the potentially large group index increase of gain in (20) is "structural,"[54] i.e., associated with the changes in the waveguide dispersion rather than due to changes in material dispersion, which do not change the gain.

6. Rate Equations, Excess Noise Factor n_{s} and Transparency Density

The rate equation (16) for photons away from the equilibrium can be written as

$$\frac{\mathrm{d}n_{\mathrm{p}}}{\mathrm{d}t} = \frac{n_2}{\tau_{\mathrm{rad,m}}} + \frac{(n_2 - n_1)n_{\mathrm{p}}}{\tau_{\mathrm{rad,m}}} - \frac{n_{\mathrm{p}}}{\tau_{\mathrm{p}}} \tag{21}$$

where τ_p is the photon lifetime in the cavity. Now, let us consider the relation between n_2 and n_1. If one operates with an ideal four level system, such as Nd^{3+} ions, then $n_1 = 0$, but if the system is not ideal, then the lower level will always have some population. For example, in case of quantum cascade laser (QCL),[55] the ratio n_2/n_1, equal to the ratio of the level lifetimes, remains constant up until threshold. Then one can introduce a so-called incomplete population inversion factor[3,56] $n_{\mathrm{s}} = n_2/(n_2 - n_1) \approx 1 - 2$ and then re-write (21), using $\tau_{\mathrm{rad}}^{-1} = \beta^{-1}\tau_{\mathrm{rad,m}}$ as

$$\frac{\mathrm{d}n_{\mathrm{p}}}{\mathrm{d}t} = \beta\frac{1 + n_{\mathrm{p}}/n_{\mathrm{s}}}{\tau_{\mathrm{rad}}}n_2 - \frac{n_{\mathrm{p}}}{\tau_{\mathrm{p}}} \tag{22}$$

We shall refer to this first type of the active medium, with constant population inversion factor, as "four level lasers" and

besides aforementioned Nd^{3+} laser and QCL it also includes Ti–Sapphire laser and Tm^{3+} laser operating at some of the transitions.[57] If, on the other hand, we consider a semiconductor diode laser, then in the absence of pumping the active medium is absorbing, and the gain can be approximated as,[56] where N_c is the injected carrier density, a is a differential gain, defined as $a = \partial g/\partial N_c$ and N_{c0} is a transparency carrier density. Typically, $N_{c0} \approx 1 \times 10^{18}\text{cm}^{-3}$. Other broad-band gain media, such as dye molecules, also exhibit absorption in the absence of pumping. Then one can re-write the rate Equation (21) as

$$\frac{dn_p}{dt} = \beta\frac{n_c}{\tau_{rad}} + \beta\frac{(n_c - n_{c0})n_p}{\tau_{rad}} - \frac{n_p}{\tau_p} \tag{23}$$

where $n_c = N_c V_a$ and V_a is the active region volume. Now the excess noise factor $n_s = n_c/(n_c - n_{nc0})$ is no longer a material constant, but depends on the value of threshold population inversion, i.e., on cavity loss. Besides semiconductors, gain media with Er^{3+} and Yb^{3+} ions as well as the ones based on dye molecules also have transparency density since lower laser level in them has finite thermal population, and their dynamics can be described by (23).

Next, we complement the rate equation for photons (22) with the rate equation for the upper level population

$$\frac{dn_2}{dt} = p - \beta\frac{1 + n_p/n_s}{\tau_{rad}}n_2 - \frac{1-\beta}{\tau_{rad}}n_2 - \frac{1-\eta_{rad}}{\tau_{rad}\eta_{rad}}n_2 \tag{24}$$

Here the first term on the r.h.s. is pumping rate p, the second term is the sum of spontaneous and stimulated emission rates into the laser mode, the third term is the spontaneous emission rate into all other modes, and the last term is nonradiative recombination rate, with the radiative efficiency defined as $\eta_{rad} = \tau/\tau_{rad}$, where $\tau^{-1} = \tau_{rad}^{-1} + \tau_{nrad}^{-1}$ is the combined radiative and nonradiative relaxation rate.

7. Lasing Threshold and Linewidth of Four Level Laser with Constant n_s

Let us find the steady state solution of (22) and (24) as

$$p = \frac{\beta n_2}{\tau_{rad}}\left[\frac{n_p}{n_s} + \beta^{-1}\eta_{rad}^{-1}\right]$$

$$\beta\frac{n_2}{\tau_{rad}} = \frac{n_p}{\tau_p(1 + n_p/n_s)} \tag{25}$$

which immediately leads us to the equation connecting the pump rate and the photon number

$$p = \frac{n_p}{\tau_p(n_s + n_p)}\left[n_p + n_s\beta^{-1}\eta_{rad}^{-1}\right] \tag{26}$$

The output photon flow can then be introduced as $r_{out} = \eta_{out}n_p/\tau_p$, where $\eta_{out} \sim T/(T + L_{other})$ is the outcoupling efficiency determined by the relative weight of mirror transmission T and other losses L_{other} The plot of Light–pump dependence $n_p(p)$ is shown in **Figure 5** for different values of β, η_{rad}, and n_s.

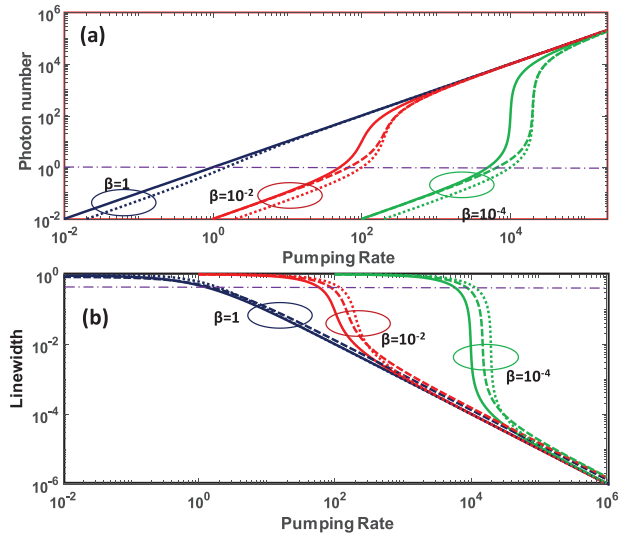

Figure 5. a) Light–pump characteristics and b) Linewidth of a four level nanolaser for different β's and radiative efficiencies (solid lines—η_{rad} = 100%, n_s = 1; dashed lines—η_{rad} = 100%, n_s = 1.5; dotted lines—η_{rad} = 50%, n_s = 1).

As one can see, for 100% radiative efficiency and $\beta = 1$, the light–pump curve is a straight line, which is easy to explain by the fact that all the pumped power has only one outlet—emission into a single mode. That is why this type of laser is often referred to as "threshold-less." This definition is obviously wrong because whether the laser is lasing or not is determined by the coherence of the emission. One may compare stimulated (i.e., coherent) photon emission with the spontaneous (i.e., incoherent) emission and postulate that threshold occurs when the stimulated emission rate surpasses the spontaneous emission rate, i.e., $n_p = n_s$. In this case, we obtain

$$p_{th} = \frac{n_s}{2\tau_p}\left[1 + 1/\beta\eta_{rad}\right] \tag{27}$$

To understand the significance of the threshold, let us derive the expression for the linewidth of the laser as the linewidth of the "hot" cavity with gain, from (22)

$$\Delta\omega_{las} = \frac{1}{\tau_p} - \frac{\beta}{n_s\tau_{rad}}n_2 \tag{28}$$

and substituting the second equation of (25) into (28) we obtain

$$\Delta\omega_{las} = \frac{n_s}{\tau_p(n_s + n_p)} \tag{29}$$

At threshold, as defined by (27), the linewidth of the laser decreases by a factor of 2. It can also be shown that the condition $n_p = n_s$ corresponds to the point where the second order autocorrelation function becomes equal to unity.[58–60] Phenomenologically, the linewidth represents the phase noise, and the phase noise is determined by the ratio of random-phase spontaneously emitted photons n_s to all the photons, including n_p coherent photons with identical phase.[61] The linewidth versus pump rate is

plotted in Figure 5b and as one can see the linewidth reduction at threshold occurs for all spontaneous emission factors, including $\beta = 1$. Obviously, the smaller is β, the sharper is the change of slope in for both photon number and linewidth of the laser.

Well below threshold ($n_p << n_s$) the dependence $n_p(p)$ is linear and one can write for the output rate $r_{out} \approx \beta\eta_{rad}\eta_{out}p$. At the same time, well above the threshold ($n_p >> n_s$), it is also linear

$$r_{out} \approx \eta_{out}\left[p - n_s/\left(\beta\eta_{rad}\tau_p\right)\right] \tag{30}$$

but with a different slope, indicating that above the threshold all the excess energy goes into the laser mode while below it the energy goes into all the modes as well into the nonradiative dissipation. Equation (30) brings us to the more familiar definition of the laser threshold as the intercept point with the horizontal axis

$$p_{th,0} = \frac{n_s}{\beta\eta_{rad}\tau_p}. \tag{31}$$

For the large cavities with $\beta << 1$, two threshold definitions, (27) and (31), differ by a factor of two while for small cavities they get closer to each other and for the ultimate case of $\beta = \eta_{rad} = 1$, they become identical. Which definition of threshold is used will not influence the conclusions of this study which, as already mentioned, is not aimed at precise estimation of laser parameters but at understanding the role played by β, F_P and Q.

8. Four Level Laser: Threshold Dependence on β and F_P

So, let us look how does the threshold defined in (27) depends on Purcell factor and β. Purcell factor dependence is implicit in the quantum efficiency—as one can write

$$\eta_{rad}^{-1} = 1 + (1 - \eta_{rad0})/\eta_{rad,0}F_P \tag{32}$$

where $\eta_{rad,0}$ is the radiative efficiency in the absence of Purcell enhancement, as illustrated in **Figure 6**. For relatively poor radiative efficiency emitters the enhancement $\eta_{rad}/\eta_{rad,0}$ can be quite significant.

Thus, using (4) we obtain for the case of large ($\beta << 1$) photonic cavity. where $F_P = 1$

$$p_{th} = \frac{n_s}{2\tau_p}\frac{\pi V'}{Q_{em}\eta_{rad,0}} \tag{33}$$

Basically, it tells us that threshold depends only on two material properties (radiative efficiency and the emission linewidth), the cavity volume, and the photon lifetime. But photon lifetime and cavity volume are not independent parameters, and we can write the expression of the photon lifetime

$$\frac{1}{\tau_p} = \frac{c}{2nL}\left(\ln\frac{1}{R_1R_2} + 2\alpha\Gamma L_a\right) = \frac{\omega}{2\pi L'}\ln\frac{1}{R_1R_2} + \alpha\frac{c}{n}\Gamma\frac{L_a'}{L'} \tag{34}$$

where the first term is due to finite mirror reflectivities R_1, R_2 and the second term is due to parasitic loss in active medium α.

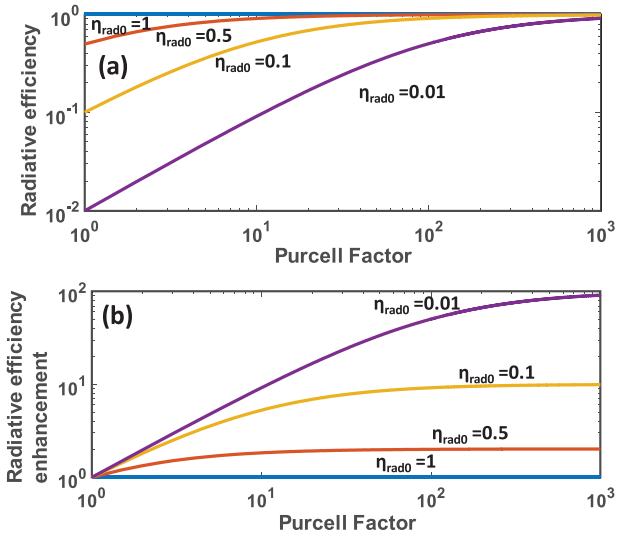

Figure 6. a) Purcell-modified radiative efficiency η_{rad} and b) Relative enhancement of radiative efficiency η_{rad}/η_{rad0} versus Purcell factor for four different values of the original, unmodified radiative efficiency $\eta_{rad,0}$.

Substituting (34) into (33), we obtain the familiar expression for the laser threshold

$$p_{th} = \frac{n_s w't'}{4}\frac{\Delta\omega}{\eta_{rad,0}}\left[\ln\frac{1}{R_1R_2} + 2\alpha\Gamma L_a\right] = \frac{n_s w't'}{2}\frac{\pi\Delta\omega}{\eta_{rad,0}F} \tag{35}$$

where F is the cavity finesse. Recommendation is rather simple—to reduce threshold, small mode area $w't'$ is always required, and if additional loss in active medium α is present, then one should reduce the volume of active medium, by either reducing confinement factor $\Gamma = w_a t_a/wt$ or the length of active medium L_a. Of course, if one looks at virtually any low threshold laser, and especially in semiconductor lasers, one always uses narrow, preferably single transverse mode waveguide and a relatively low confinement factor. Since the smallest mode area of the photonic laser is on the scale of $(\lambda/n)^2$, the minimum threshold is determined only by the spectral width of spontaneous emission, cavity losses and radiative efficiency, with β nowhere found explicitly. Clearly, one can increase the cavity length L and thus reduce β without affecting threshold, but increasing the mode area will increase the threshold.

Similarly, by increasing the cavity length, one can increase the cavity Q-factor, without reducing the threshold, as has been shown in Figure 1. This denounces another popular myth in nanolaser lore that increase of the Q-factor necessarily reduces the laser threshold. In fact, threshold depends on the product $Q_{cav}\beta$, which is proportional to finesse of the cavity, and does not change with change of length, because this product is nothing but inverse of cavity loss, so it makes little sense to talk about β and Q separately. Of course, in practical lasers the active volume is typically determined by the power requirements and the heat removal considerations, while the cavity length is determined by the desired beam quality, by necessity to accommodate intracavity components, as well as by the linewidth, and not just by threshold reduction, hence invoking either β or Purcell factor for large lasers is basically irrelevant.

Next we consider 2D plasmonic cavity with large β defined in (5) and Purcell factor (12). The threshold pump rate is then

$$p_{\rm th} = \frac{n_{\rm s} n_{\rm e}' w'}{4} \frac{\Delta\omega}{\eta_{\rm rad0}} \left[\ln \frac{1}{R_1 R_2} + 2\alpha n_{\rm g}' \Gamma L_{\rm a} + \alpha_{\rm m} L \right] \times \left[\eta_{\rm rad0} + \frac{t'}{n_{\rm e}' n_{\rm g}'} (1 - \eta_{\rm rad0}) \right] \tag{36}$$

where $\alpha_{\rm m}$ is the loss in the metal. The threshold depends now mostly on the width of the mode and confinement factor, just as for a 3D photonic cavity, but for the lasers with low radiation efficiency, it can be reduced for the case of very thin gap between two metal plates. However, the metal loss increases as the thickness of waveguide decreases as roughly[25]

$$\alpha_{\rm m} \approx 2 \frac{n\gamma}{c} \frac{\omega}{\omega_{\rm p}} \frac{1}{t'} \tag{37}$$

where γ is scattering time in metal, and $\omega_{\rm p}$ is the plasma frequency. As one can see, the metal loss becomes less significant for lower frequencies.[24] Therefore, in practical sense, reduction of size thickness below diffraction limit can only be helpful to lower threshold in metal-clad quantum cascade lasers operating in the terahertz (THz) region of spectra[62,63] because the radiative efficiency of inter-subband transitions is extremely low and the metal loss in THz region is reduced as the field only weakly penetrates metal at these frequencies.

For the 1D plasmonic waveguide, the expression for the threshold is similarly obtained using (6) and (13)

$$p_{\rm th} = \frac{n_{\rm s}}{2\pi} \frac{\Delta\omega}{\eta_{\rm rad,0}} \left[\ln \frac{1}{R_1 R_2} + 2\alpha n_{\rm g}' \Gamma L_{\rm a} + \alpha_{\rm m} L \right] \times \left[\eta_{\rm rad0} + \frac{S'}{n_{\rm g}'} (1 - \eta_{\rm rad0}) \right] \tag{38}$$

and as one can see that neither increase in β nor increase in the Purcell factor can reduce the threshold that depends mostly on the value of confinement factor and the metal loss.

If one now takes a deeper look into what physical processes Equations (35)–(38) connote, one may grasp that Purcell factor cannot be unequivocally considered to play a beneficial role. According to (35), reduction of the transverse size of the cavity causes commensurate decrease in the threshold, but it works only for as long as $w', t' > 1$ after that reduction of the volume that needs to be pumped is accompanied by the equal reduction in radiative lifetime, hence if the radiative decay is the only relaxation process, the threshold no longer changes with transverse size as can be seen from (36) and (38) with $\eta_{\rm rad0} = 1$. It is only when radiative efficiency is low, as in aforementioned THz QCL that the deleterious impact of Purcell enhancement of spontaneous decay becomes less important and reduction of the transverse size beyond diffraction limit continues to reduce the threshold. The fact that Purcell factor happens to increase as the transverse size gets smaller cannot be construed in a way that Purcell factor is responsible for the threshold reduction, just as the strong motions of the trees in a hurricane-strength wind cannot be held responsible for all the damage inflicted by the storm.

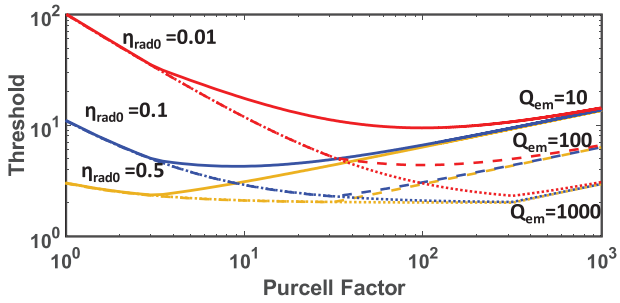

Figure 7. Threshold reduction due to Purcell enhancement of radiative efficiency for different values of radiative efficiency in the unconstrained dielectric $\eta_{\rm rad0}$ and emission linewidth.

But what if the volume is small and $\beta = 1$? Then, since the Purcell enhancement is the same for all cavities, the expression for threshold pumping rate is the same for all cavities

$$p_{\rm th} = \frac{n_{\rm s}}{2\tau_{\rm p}} \left[1 + 1/\eta_{\rm rad} \right] = \frac{n_{\rm s}}{2\tau_{\rm p}} \left[2 + \frac{(1 - \eta_{\rm rad0})\, \pi V'}{\eta_{\rm rad0} Q_{\rm em}} \right] \tag{39}$$

Therefore, unless one operates with very low quantum efficiency then at best, i.e., assuming that photon lifetime is independent on the dimensions, the threshold does not change with the dimensions. At worst, the photon lifetime actually decreases with the cavity size. For example, if one is using a ring, or micro disc WGM resonator,[44] the bending loss goes up exponentially as the radius decreases. For the vertical cavity surface emitting geometry, the diffraction loss also increases as the area decreases,[64] and, of course, photon lifetime decreases when the cavity gets shorter. And if the metal is involved, the loss increases with volume as the field gets more and more inside the metal.[26,65] Let us write, in very general terms, for a small cavity $V \le (\lambda/2n)^3$

$$\tau_{\rm p} = \tau_{\rm p}^{(\rm dif)} \left(V' \right)^{1/3} = \tau_{\rm p}^{(\rm dif)} \left(Q_{\rm em}/\pi F_{\rm p} \right)^{1/3} \tag{40}$$

where $\tau_{\rm p}^{(\rm dif)}$ is the value of the photon lifetime, when the size of cavity is larger than the diffraction limit, i.e., $V > (\lambda/2n)^3$. Then, the threshold pump rate becomes

$$p_{\rm th} = p_{\rm th}^{(0)} \left(\frac{\pi F_{\rm p}}{Q_{\rm em}} \right)^{1/3} \left(2 + \frac{1 - \eta_{\rm rad0}}{\eta_{\rm rad0} F_{\rm p}} \right) \tag{41}$$

where $p_{\rm th}^{(0)} = n_{\rm s}/2\tau_{\rm p}^{(\rm dif)}$. The threshold pump rate normalized to $p_{\rm th}^{(0)}$ is plotted in **Figure 7** as a function of Purcell factor for three different values of un-enhanced radiative efficiency $\eta_{\rm rad0}$ and three different values emission linewidths, i.e., $Q_{\rm em}$

As one can see, the reduction of threshold is significant only for the gain material with low quantum efficiency, In fact, for $\eta_{\rm rad0} > 0.5$, the reduction of threshold is less than 30%, no matter how narrow the emission linewidth is. For lower quality materials, the decrease of the threshold may be more substantial, but the minimum of threshold always occurs at the value of Purcell factor less than $Q_{\rm em}/\pi$, corresponding to $V \ge (\lambda/2n)^3$, i.e., never below the diffraction limit. This fact makes photonic cavity preferable to subdiffraction limit plasmonic cavity. In plasmonic cavity (15), Purcell factor is determined by the cavity quality factor $Q_{\rm cav} = \omega\tau_{\rm p}$

and (39) becomes

$$p_{\rm th} = \frac{n_{\rm s}}{2\tau_{\rm p}}\left[2 + \frac{\left(1-\eta_{\rm rad0}\right)\pi V'}{\eta_{\rm rad0}\omega\tau_{\rm p}}\right] \approx p_{\rm th}^{(0)}\left[\frac{1}{(V')^{1/3}} + \frac{\left(1-\eta_{\rm rad0}\right)\pi (V')^{1/3}}{\eta_{\rm rad0}Q_{\rm cav}^{(\rm dif)}}\right] \quad (42)$$

where $Q_{\rm cav}^{(\rm dif)} = \omega\tau_{\rm p}^{(\rm dif)}$. This expression has minimum at $(V')^{1/3} = \sqrt{\eta_{\rm rad0}Q_{\rm cav}^{(\rm dif)}/(1-\eta_{\rm rad0})\pi}$ and $F_{\rm P} = (1-\eta_{\rm rad0})/\eta_{\rm rad0}$, with minimum threshold equal to

$$p_{\rm th,min} = 2p_{\rm th}^{(0)}\sqrt{\frac{\left(1-\eta_{\rm rad0}\right)\pi}{\eta_{\rm rad0}Q_{\rm cav}^{(\rm dif)}}} \quad (43)$$

Therefore, any threshold reduction is possible only if $\eta_{\rm rad0}Q_{\rm E}^{(\rm dif)} < 1/4\pi$, i.e., since $Q_{\rm cav}^{(\rm dif)} > 10$, the radiative efficiency has to be less than 1% to see a positive impact of volume decrease, which, once again brings us to the case of mid-IR and especially THz QCL's where the lasers with subwavelength volumes has been indeed demonstrated.[66,67] One can then make an interesting observation: in single mode lasers the threshold can only be decreased if the gain media has such a low radiative efficiency that spontaneous emission and Purcell factor are simply irrelevant!

Overall, one can observe beneficial effect of volume reduction beyond the diffraction limit only in systems with very low quantum efficiency, but in many of these systems one can never reach threshold in small cavity precisely because of the low quantum efficiency. At any rate, most of the laser media today has high quantum efficiency, hence, clearly Purcell enhancement does not do anything to reduce threshold. More conclusions about impact of Purcell factor will be made at the end of Section 10, after the most interesting case of semiconductor lasers is considered.

9. Lasing Threshold and Linewidth of Semiconductor and Other Lasers with Transparency Carrier Density N_{c0}

Let us now move on to a more relevant case of the lasers based on the media, in which the transparency density N_{c0} is present, such as semiconductors. Although as mentioned above, other laser media in which energy levels are split into the manifolds resembling energy band in semiconductors (e.g., dye molecules,[68] ruby, or Er^{3+} and Yb^{3+} ions[69,70]) also fit into the same group, it is semiconductor nanolasers, especially injection pumped ones that arouse interest from the application point of view.[56] The steady state balance Equations (23) and (24) for this case are

$$\beta\frac{n_{\rm c}}{\tau E} + \beta\frac{(n_{\rm c}-n_{\rm c0})n_{\rm p}}{\tau_{\rm rad}} - \frac{n_{\rm p}}{\tau_{\rm p}} = 0$$

$$p = \frac{\beta n_{\rm c}}{\tau_{\rm rad}}\left[n_{\rm p} + \beta^{-1}\eta_{\rm rad}^{-1}\right] - \frac{\beta n_{\rm c0}n_{\rm p}}{\tau_{\rm rad}} \quad (44)$$

and their solution is

$$p = \frac{n_{\rm p}}{(1+n_{\rm p})\tau_{\rm p}}\left[n_{\rm p} + \beta^{-1}\eta_{\rm rad}^{-1}\right] + \frac{n_{\rm p}n_{\rm c0}}{(1+n_{\rm p})\tau_{\rm rad}\eta_{\rm rad}}\left[1-\beta\eta_{\rm rad}\right] \quad (45)$$

The second term on the r.h.s. of (45) is obviously positive and, therefore, increases with decrease of the radiative time, hence, one cannot expect the Purcell factor to play a beneficial role there. The first term, however, has radiative efficiency included in it, and, therefore, can be reduced by Purcell enhancement of radiative decay. One can introduce a new parameter—the ratio of the loss due to saturable absorption to the loss due to mirror transmission and scattering

$$s = \beta n_{\rm c0}\tau_{\rm p}/\tau_{\rm rad} \quad (46)$$

and re-write (45) as

$$p = \frac{n_{\rm p}}{(1+n_{\rm p})\tau_{\rm p}}\left[n_{\rm p} + \beta^{-1}\eta_{\rm rad}^{-1}[1+s(1-\beta\eta_{\rm rad})]\right] \quad (47)$$

Well below threshold ($n_{\rm p} << 1$), the dependence $n_{\rm p}(p)$ is linear and one can write for the output rate $r_{\rm out} \approx \beta\eta_{\rm rad}\eta_{\rm out}p[1+s(1-\beta\eta_{\rm rad})]^{-1}$, while well above threshold ($n_{\rm p} >> 1$) it is also linear, $r_{\rm out} \approx \eta_{\rm out}(p-p_{\rm th,0})$, with the threshold pump rate defined as

$$p_{\rm th,0} = \frac{1+s(1-\beta\eta_{\rm rad})}{\beta\eta_{\rm rad}\tau_{\rm p}} \quad (48)$$

Obviously the expression in the numerator plays the role of the excess noise factor $n_{\rm s}$ in (31), even though it depends on photon lifetime, i.e., it is not solely a material property.

The dependence of photon density versus pump rate is shown in **Figure 8**a. for different values of $\beta\eta_{\rm rad}$ and three different values of s.

The expression for a linewidth can be obtained from the first equation in (44) following the procedure outlined in Section 7

$$\Delta\omega_{\rm las} = \frac{1+s}{\tau_{\rm p}(1+n_{\rm p})} \quad (49)$$

as plotted in Figure 8b. Since $(1+s)/\tau_{\rm p}$ is the linewidth in the absence of pumping, $n_{\rm p} = 1$ can be considered to be a lasing threshold and then from (47) it follows that

$$p_{\rm th} = \frac{1}{2\tau_{\rm p}}\left[1 + \beta^{-1}\eta_{\rm rad}^{-1}[1+s(1-\beta\eta_{\rm rad})]\right] \quad (50)$$

Just as in Section 7, two definitions of threshold (48) and (50) are identical for cavity with $\beta\eta_{\rm rad} = 1$ and differ by a factor of two for large cavities with $\beta << 1$. The curves in Figure 8 are similar to those in Figure 5 for a four-level laser. Once again, for $\beta\eta_{\rm rad} = 1$, the light–pump characteristics is a straight line, but the linewidth dependence clearly shows the threshold. It is also clear that in order to achieve narrow linewidth without having excessive pump density, one needs to use the small β, or, essentially lasers with large volumes so that the cavity can store large number of coherent photons.

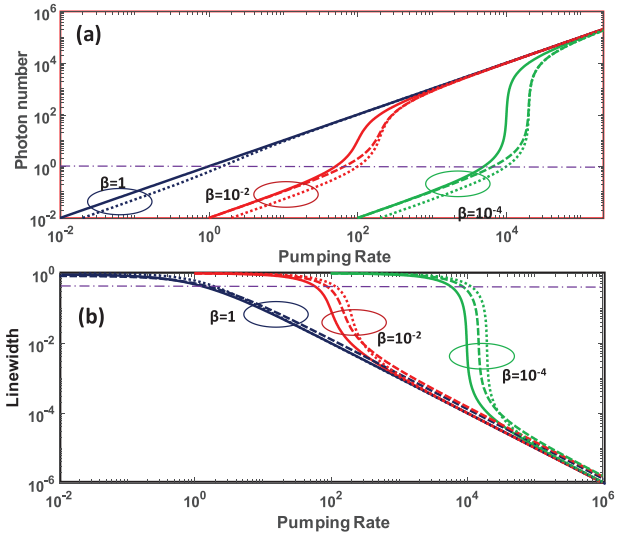

Figure 8. a) Light–pump characteristics. b) Linewidth (normalized to linewidth of the empty cavity) of a semiconductor nanolaser for different values of $\beta\eta_{rad}$ product and the saturable loss ratios (solid lines $s = 0.1$; dashed lines $s = 1$, $n_s = 1.5$; dotted lines $s = 10$). Pumping rate is in units of $1/\tau_p$.

10. Semiconductor Laser: Threshold Dependence on β and F_P

Let us now consider how the spontaneous emission factor affects the threshold of semiconductor nanolaser. From (50) and (46), under assumption $\beta << 1$ for the large 3D cavity, we obtain

$$p_{th} = \frac{1}{2\tau_p \beta \eta_{rad}} + \frac{n_{c0}}{\eta_{rad}\tau_{rad}}$$
$$= \frac{n^2 wt}{\lambda^2}\frac{\Delta\omega}{\eta_{rad}}\left[\ln\frac{1}{R_1R_2} + 2\alpha\Gamma L_a\right] + \frac{N_{c0}}{\tau_{rad}\eta_{rad}} wt\Gamma L_a$$
$$= \frac{n^2 wt}{\lambda^2}\frac{\Delta\omega}{\eta_{rad}}\left[\ln\frac{1}{R_1R_2} + 2\alpha\Gamma L_a + \Gamma\frac{\lambda^2}{n^2}\frac{N_{co}L_a}{\Delta\omega\tau_{rad}}\right] \quad (51)$$

Note that threshold has two contributions—one from the cavity loss and one from the necessity to maintain population inversion above transparency.[36] Obviously, small mode volume tends to reduce threshold, but one cannot say that any increase in β will automatically cause the threshold decrease. First of all, increase in the cavity length is not going to change the threshold, as long as the length of active region L_a remains constant (as expected from the exercise in Figure 1). Only the change of cross-section affects the threshold and that is why single mode waveguide is the dominant mean of photon confinement in the semiconductor lasers. But with large transparency carrier density, it is the dimensions of the active region that is most relevant to the threshold—that is why typical semiconductor laser incorporates no more than a few active quantum wells and has a very small confinement factor. Once again, the purpose of this work is not to educate semiconductor laser engineers on the strategies for achieving low threshold—they have mastered this art long ago without invoking concepts of β and F_p. Actual value of confinement factor and mode size are, of course, determined not only by a desire to reduced threshold, but also by the necessity of extracting certain power from the laser without causing optical or thermal damage.

For the 2D plasmonic waveguide cavity one obtains, in analogy with (36)

$$p_{th} = \frac{nn_e' w}{2\lambda}\frac{\Delta\omega}{\eta_{rad0}}\left[\ln\frac{1}{R_1R_2} + 2\alpha n_g'\Gamma L_a + \alpha_m L + \Gamma\left(\frac{2\lambda}{n}\right)^2\frac{N_{co}L_a n_e' n_g'}{\Delta\omega\tau_{rad0}}\right]\left[\eta_{rad0} + \frac{t'}{n_e' n_g'}(1-\eta_{rad0})\right] \quad (52)$$

and for the plasmonic waveguide, in analogy with (38)

$$p_{th} = \frac{1}{2\pi}\frac{\Delta\omega}{\eta_{rad,0}}\left[\ln\frac{1}{R_1R_2} + 2\alpha n_g'\Gamma L_a + \alpha_m L + \Gamma 2\pi\left(\frac{2\lambda}{n}\right)^2\frac{N_{co}n_g' L_a}{\Delta\omega\tau_{rad0}}\right] \times\left[\eta_{rad0} + \frac{S'}{n_g'}(1-\eta_{rad0})\right] \quad (53)$$

For as long as radiative efficiency is high, as is the case for most semiconductors operating in the visible and near IR, the threshold gets reduced with the reduction volume of active medium rather than with the volume of the cavity, and thus, as we have already discussed, will have very little to do with the Purcell factor. Of course, reducing the volume of active medium means pumping more power into the smaller volume, which can cause overheating as well as gain saturation. Only if the radiative efficiency is relatively poor which may be the case for semiconductor lasers operating in mid-IR[71] (due to Auger recombination), or near-IR and mid-IR transitions in rare earth ions (such as Er^{3+},[72,73] Tm^3,[74] Ho^{3+},[75,76] Dy^3[77,78] one may expect the impact of cavity transverse size reduction be positive. But even at those frequencies, the increase of the metal loss may actually increase the threshold and only the experimental work will provide a definitive answer.

For a small cavity with $\beta = 1$, one obtains from (50)

$$p_{th} = \frac{1}{2\tau_p}\left[2 + (s+1)(\eta_{rad}^{-1} - 1)\right] \quad (54)$$

Using (46) and (32) this can be re-worked as

$$p_{th} = \frac{1}{2\tau_p}\left[2 + \left(n_{co}\frac{\tau_p}{\tau_{rad}} + 1\right)\frac{1-\eta_{rad0}}{\eta_{rad0}F_P}\right] \quad (55)$$

Typically, in a semiconductor laser the radiative efficiency is very close to unity, so that threshold power is simply the quantum limit, $p_{th} \approx 1/\tau_p$. For the smaller quantum efficiencies, we can once again assume that the photon lifetime gets reduced when the volume becomes subdiffraction, according to (40), and assuming that the confinement factor is volume independent

$$p_{th} = p_{th}^{(0)}\left(\frac{\pi F_P}{Q_{cav}}\right)^{1/3}\left(2 + \frac{1-\eta_{rad0}}{\eta_{rad0}F_P}\right) + \Gamma\frac{Q_{cav}N_{c0}}{\pi F_P\tau_{rad0}}\left(\frac{\lambda}{2n}\right)^3\frac{1-\eta_{rad0}}{\eta_{rad0}} \quad (56)$$

where $r = \Gamma Q_{em} N_{c0} (\lambda/2n)^3 \tau_p^{(dif)}/\pi\tau_{rad}$. For typical values of $N_{c0} = 10^{18}\text{cm}^{-3}$, $\lambda = 1\ \mu\text{m}$, $n = 3$, $Q_{cav} \approx 10, \tau_p^{(dif)} = 100\,\text{fs}$ and $\tau_{rad0} = 1\,\text{ns}$, the last term dominates, indicating that whatever reduction of threshold can be achieved is small cavities, it is mostly due to decrease of the active volume, and not due to increase in the radiative recombination rate. Once again, this exercise is mostly hypothetical for the semiconductor lasers because the radiative recombination efficiencies in today's semiconductor lasers always exceed 90%. It may be more relevant for laser dyes. Also, the value of the threshold at the quantum limit for the dielectric cavities may be sufficiently small, but for the subwavelength plasmonic cavities photon lifetime is on order of the electron scattering time in metals, i.e., 10 fs. It means that the pump power is at the very least $\hbar\omega/\tau_p \approx 20\ \mu\text{W}$ for the near IR. For the 100 nm subdiffraction volume this power corresponds to power density of $20\,\text{GWcm}^{-3}$ making CW lasing unsustainable due to overheating.

Overall, a plasmonic cavity which is subwavelength in one or two dimensions[6,36,79] but longer than wavelength along the light propagation direction is much better poised for threshold reduction than a spaser[10] that is subwavelength in all three dimensions. Such elongated cavity can be MIM waveguide,[12,28] or hybrid nanowire cavity.[38] It obviously has $\beta \ll 1$ and a rather modest Purcell factor, but the loss in such a cavity may not be prohibitively high in the mid-to-far IR region.

11. Conclusions

So, what conclusions can be drawn from this rather long discourse? Before making them, we shall re-emphasize that this work does not claim to offer any guidance to the design of practical micro and nanolasers. To say otherwise would be an affront to all the scientists and engineers who have dedicated their lives to design of practical lasers and have achieved amazing successes, having overcome plenty of obstacles on the way. The modest goal of this work was simply to determine whether including spontaneous emission factor β, the Q factor, and Purcell factor F_P into consideration is helpful or not? Obviously, talking about all of these factors in itself cannot hurt. Moreover, β can be conveniently used to explain why both power and coherence of large lasers experience sharp increase at the threshold, while for small lasers the change is not all that pronounced. And Purcell factor may be invoked to discuss radiative lifetime shortening and ensuing increase of modulation speed of the laser. (As a useful footnote, it should be mentioned that for practical applications such as high capacity interconnects a certain power is required just to achieve error free detection without amplifiers and energy consuming forward error correction. This power is as high as a few tens of microwatts for 100s of gigabits per second throughput.[80] Hence special attention must be given to assuring that nanolaser can operate continuously at high power density.)

What is not prudent in our view is to develop a mode of thinking in which increase of β-factor, quality factor Q_{cav}, or Purcell factor F_P unequivocally implies the reduction of threshold or other power-related improvements.

In **Figure 9** we sketch the relation (or lack of such) between β, F_P and threshold power (relative units) under simplifying assumptions of constant confinement factor. The threshold power

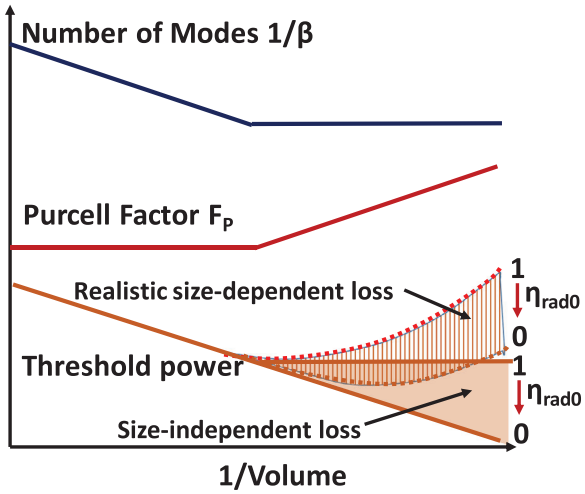

Figure 9. A sketch (on the logarithmic scale) of the evolution of spontaneous emission factor, Purcell factor, and threshold power of a laser with a cavity volume. Solid lines assume volume independent cavity loss, while dashed lines assume more realistic case of loss increasing for smaller volumes.

is plotted for the range of radiative efficiencies η_0 from 1 to approaching 0, and for the two cases—one in which cavity loss remains unchanged with cavity size (solid lines), and the other, a more realistic one, for which the radiative and/or nonradiative loss increases as cavity gets smaller dashed lines) . Note that the threshold curve represents just a trend, and the absolute value of the threshold power increases inversely proportional to η_{rad0}^{-1}

When it comes to spontaneous emission factor β, generally its increase, indeed, coincides with the reduction of the threshold power, but claiming that the reduction of threshold is caused by the increase of β is putting the cart ahead of the horse. The reduction of the threshold for the most part is associated simply with the reduction of the active volume of the laser, especially if the active medium is a semiconductor with large transparency carrier density and large intracavity loss caused by free carrier absorption. The cavity cross-section follows the decrease of the cross-section of the active medium in order to keep confinement factor reasonably high, so β increases, but it would be erroneous to say that threshold decrease is caused by increase of β. Furthermore, changing the cavity length while keeping the active volume constant will not change the threshold despite the change of β factor and cavity Q-factor. In the end, laser threshold per unit area of the mode depends only on the emission linewidth $\Delta\omega$, cavity finesse F (i.e., loss), and radiative quantum efficiency η_{rad}[81] and there is no need to invoke any other quantity to explain this.

When it comes to the Purcell factor, it is important to understand that both stimulated and spontaneous emission rates get affected equally, hence, for the active medium with high radiative efficiency Purcell factor is not going to affect threshold at all. The increase in the stimulated emission rate will be completely balanced by the decrease of the upper laser lifetime, hence τ_{rad} is absent from all the threshold expressions derived in this study, e.g. (27), (31), (48), and (50). This can be clearly seen in Figure 8, where in the ideal case of $\eta_0 = 1$ and size-independent loss the thresholds gets clamped and does not decrease as Purcell factor

increases. Only for the gain medium with a very poor radiative efficiency, where the upper laser lifetime is not going to decrease by too much with the enhancement of radiative rate, one can expect any significant improvement occurring concurrently with Purcell enhancement. But as we have discussed at length, occurring "concurrently" does not mean occurring "as a consequence of." The threshold reduction simply follows decrease in volume one has to pump, and, if anything, Purcell effect acts as a spoiler that reduces the upper laser state lifetime. Only when radiative efficiency is extremely poor, i.e., radiative decay of upper state (and therefore Purcell effect) are no longer relevant, the threshold reduction can be attained with reducing the dimensions of laser beyond diffraction limit. Of course, if the cavity loss increases with the decrease of volume toward and beyond the diffraction limit, as is usually the case, the threshold reverses its downward trend and starts growing with Purcell factor as one can see from the dashed curves in Figure 9.

At any rate, if the radiative efficiency is poor (as in quantum cascade laser) it is highly unlikely that laser threshold can, indeed, be attained in a significantly subwavelength volume where Purcell effect becomes very large. Prospects are better for the "long" plasmonic lasers that are subwavelength in only one or two dimensions and thus have relatively small Purcell factor, on the order of a few. But of course, it should be taken into account that under realistic conditions the decrease in size is always accompanied by the increase of loss.[36,65] Therefore, if subwavelength dimension offers a benefit, it should be sought in the mid and far infrared and THz regions, where the losses are reduced and many laser materials have low radiative efficiency. Note though that in mid-infrared loss in the metal is so high that all the lasers there still use conventional photonic waveguides. Only in THz region metal waveguides with subwavelength thickness have been widely used, and the main reason for it the simple fact that it is difficult to grow QCL active layers with thickness of tens of micrometers.

Overall, the value of laser threshold is determined by cavity loss, radiative efficiency, emission bandwidth, and, what is most relevant for this discourse, the volume of active medium, as smaller lasers tend to require less power than the large ones, which is not exactly a groundbreaking discovery. Of course, one cannot decrease the active volume indefinitely as eventually the pump power density will become very large causing overheating and/or damage. Furthermore, if the laser is electrically pumped, the current density eventually becomes impossible to maintain.

To summarize, the cavity volume generally (but not necessarily) increases and decreases with the active medium volume and that causes changes in β, Q, and F_P, which happen to be collateral effects rather than sources of laser threshold change. Even though, as stated above, we are not offering a "design guide" for improving performance of nanolasers, we guardedly express hope that clarification of the roles played (or rather not played) by β, Q, and F_P will help understanding of this fascinating topic.

Acknowledgements

This work was supported by the NSF EiR grants 1830886 and 1856515, DoD grant W911NF1810472, and AFOSR grants FA9550-18-1-0417 and FA9550-16-10362.

Conflict of Interest

The authors declare no conflict of interest.

Keywords

laser characteristics, lasing threshold, Purcell factor

Received: June 17, 2020
Revised: November 28, 2020
Published online:

[1] C. C. Davis, *Lasers and Electro-Optics*, 2nd ed., Cambridge University Press, Cambridge; New York **2014**, p. 867.
[2] J. Hecht, *Understanding Lasers: An Entry-Level Guide*, IEEE Press, New York **1992**, p. 433.
[3] A. Yariv, P. Yeh, A. Yariv, *Photonics: Optical Electronics in Modern Communications*, 6th ed. The Oxford Series in Electrical and Computer Engineering, Oxford University Press, New York **2007**, p. 836.
[4] K. Iga, *Jpn. J. Appl. Phys.* **2018**, *57*, 08PA01.
[5] J. Pozo, E. Beletkaia, *PhotonicsViews* **2019**, *16*, 21.
[6] R.-M. Ma, R. F. Oulton, *Nat. Nanotechnol.* **2019**, *14*, 12.
[7] K. Nozaki, T. Ide, J. Hashimoto, W.-H. Zheng, T. Baba, *Electron. Lett.* **2005**, *41*, 843.
[8] K. Nozaki, S. Kita, T. Baba, *Opt. Express* **2007**, *15*, 7506.
[9] M. A. Noginov, G. Zhu, A. M. Belgrave, R. Bakker, V. M. Shalaev, E. E. Narimanov, S. Stout, E. Herz, T. Suteewong, U. Wiesner, *Nature* **2009**, *460*, 1110.
[10] D. J. Bergman, M. I. Stockman, *Phys. Rev. Lett.* **2003**, *90*, 027402.
[11] R. F. Oulton, V. J. Sorger, T. Zentgraf, R.-M. Ma, C. Gladden, L. Dai, G. Bartal, X. Zhang, *Nature* **2009**, *461*, 629.
[12] M. T. Hill, Y.-S. Oei, B. Smalbrugge, Y. Zhu, T. De Vries, P. J. Van Veldhoven, F. W. M. Van Otten, T. J. Eijkemans, J. P. Turkiewicz, H. De Waardt, E. J. Geluk, S.-H. Kwon, Y.-H. Lee, R. Nötzel, M. K. Smit, *Nat. Photonics* **2007**, *1*, 589.
[13] M. Khajavikhan, A. Simic, M. Katz, J. H. Lee, B. Slutsky, A. Mizrahi, V. Lomakin, Y. Fainman, *Nature* **2012**, *482*, 204.
[14] B. Romeira, A. Fiore, *Proc. IEEE* **2020**, *108*, 735.
[15] Q. Zhang, X. L. Zhu, Y. Y. Li, J. W. Liang, T. R. Chen, P. Fan, H. Zhou, W. Hu, X. J. Zhuang, A. L. Pan, *Laser Photonics Rev.* **2016**, *10*, 458.
[16] H. Zhou, M. Wissinger, J. Fallert, R. Hauschild, F. Stelzl, C. Klingshirn, H. Kalt, *Appl. Phys. Lett.* **2007**, *91*, 181112.
[17] S. Wu, S. Buckley, J. R. Schaibley, L. Feng, J. Yan, D. G. Mandrus, F. Hatami, W. Yao, J. Vučković, A. Majumdar, X. Xu, *Nature* **2015**, *520*, 69.
[18] J. Y. Suh, C. H. Kim, W. Zhou, M. D. Huntington, D. T. Co, M. R. Wasielewski, T. W. Odom, *Nano Lett.* **2012**, *12*, 5769.
[19] P. Molina, E. Yraola, M. O. Ramírez, C. Tserkezis, J. L. Plaza, J. Aizpurua, J. Bravo-Abad, L. E. Bausá, *Nano Lett.* **2016**, *16*, 895.
[20] D. Liang, M. Fiorentino, T. Okumura, H.-H. Chang, D. T. Spencer, Y.-H. Kuo, A. W. Fang, D. Dai, R. G. Beausoleil, J. E. Bowers, *Opt. Express* **2009**, *17*, 20355.
[21] M. W. Kim, P.-C. Ku, *Appl. Phys. Lett.* **2011**, *98*, 131107.
[22] Q. Zhang, S. T. Ha, X. Liu, T. C. Sum, Q. Xiong, *Nano Lett.* **2014**, *14*, 5995.
[23] S. Matsuo, K. Takeda, *Photonics* **2019**, *6*, 82.
[24] J. B. Khurgin, *Opt. Express* **2015**, *23*, 4186.
[25] J. B. Khurgin, *Philos. Trans. R. Soc., A* **2017**, *375*, 20160068.
[26] J. B. Khurgin, *Nat. Nanotechnol.* **2015**, *10*, 2.
[27] J. B. Khurgin, G. Sun, *Nat. Photonics* **2014**, *8*, 468.
[28] M. T. Hill, M. Marell, E. S. P. Leong, B. Smalbrugge, Y. Zhu, M. Sun, P. J. Van Veldhoven, E. J. Geluk, F. Karouta, Y.-S. Oei, R. Nötzel, C.-Z. Ning, M. K. Smit, *Opt. Express* **2009**, *17*, 11107.

[29] S.-W. Chang, T.-R. Lin, S. L. Chuang, *Opt. Express* **2010**, *18*, 15039.
[30] M. A. Noginov, G. Zhu, M. Bahoura, J. Adegoke, C. Small, B. A. Ritzo, V. P. Drachev, V. M. Shalaev, *Appl. Phys. B* **2007**, *86*, 455.
[31] N. M. Lawandy, *Appl. Phys. Lett.* **2004**, *85*, 5040.
[32] S. Gwo, C.-K. Shih, *Rep. Prog. Phys.* **2016**, *79*, 086501.
[33] C.-Z. Ning, *Adv. Photonics* **2019**, *1*, 014002.
[34] O. Hess, J. B. Pendry, S. A. Maier, R. F. Oulton, J. M. Hamm, K. L. Tsakmakidis, *Nat. Mater.* **2012**, *11*, 573.
[35] S. I. Azzam, A. V. Kildishev, R.-M. Ma, C.-Z. Ning, R. Oulton, V. M. Shalaev, M. I. Stockman, J.-L. Xu, X. Zhang, *Light: Sci. Appl.* **2020**, *9*, 90.
[36] S. Wang, X.-Y. Wang, B. o. Li, H.-Z. Chen, Y. I.-L. Wang, L. Dai, R. F. Oulton, R.-M. Ma, *Nat. Commun.* **2017**, *8*, 1889.
[37] A. Krasnok, A. Alù, *Proc. IEEE* **2020**, *108*, 628.
[38] C. Li, Z. Liu, J. Chen, Y. Gao, M. Li, Q. Zhang, *Nanophotonics* **2019**, *8*, 2091.
[39] Z. Wang, X. Meng, A. V. Kildishev, A. Boltasseva, V. M. Shalaev, *Laser Photonics Rev.* **2017**, *11*, 1700212.
[40] R. F. Oulton, *Mater. Today* **2012**, *15*, 26.
[41] F. Lohof, R. Barzel, P. Gartner, C. Gies, *Phys. Rev. Appl.* **2018**, *10*, 054055.
[42] M. Lončar, T. Yoshie, A. Scherer, P. Gogna, Y. Qiu, *Appl. Phys. Lett.* **2002**, *81*, 2680.
[43] K. Y. Yang, D. Y. Oh, S. H. Lee, Q. I.-F. Yang, X. U. Yi, B. Shen, H. Wang, K. Vahala, *Nat. Photonics* **2018**, *12*, 297.
[44] T. Baba, D. Sano, *IEEE J. Sel. Top. Quantum Electron.* **2003**, *9*, 1340.
[45] N. Gregersen, T. Suhr, M. Lorke, J. Mørk, *Appl. Phys. Lett.* **2012**, *100*, 131107.
[46] W. Wei, X. Yan, X. Zhang, *Sci. Rep.* **2016**, *6*, 33063.
[47] D. G. Deppe, H. Huang, *Appl. Phys. Lett.* **1999**, *75*, 3455.
[48] Q. Gu, B. Slutsky, F. Vallini, J. S. T. Smalley, M. P. Nezhad, N. C. Frateschi, Y. Fainman, *Opt. Express* **2013**, *21*, 15603.
[49] B. Romeira, A. Fiore, *IEEE J. Quantum Electron.* **2018**, *54*, 1.
[50] R. Loudon, 3rd ed. *Oxford Science Publications*, Oxford University Press, Oxford; New York **2000**, p. 438.
[51] E. M. Purcell, *Proc. Am. Phys. Soc. Phys. Rev.* **1946**, *69*, 674.
[52] F. Johannes, R. Nicholas, N. Prineha, *Nanophotonics* **2018**, *7*, 1479.
[53] H. Deng, G. Weihs, D. Snoke, J. Bloch, Y. Yamamoto, *Proc. Natl. Acad. Sci. USA* **2003**, *100*, 15318.
[54] J. B. Khurgin, *Adv. Opt. Photonics* **2010**, *2*, 287.
[55] J. R. M. Faist, *Quantum Cascade Lasers*, Ist ed. Oxford University Press, Oxford United Kingdom **2013**, p. 306.
[56] L. A. Coldren, S. W. Corzine, *Diode Lasers and Photonic Integrated Circuits*, Wiley Series in Microwave and Optical Engineering, Wiley, New York **1995** p. 594.
[57] R. C. Sharp, D. E. Spock, N. Pan, J. Elliot, *Opt. Lett.* **1996**, *21*, 881.
[58] G. Björk, A. Karlsson, Y. Yamamoto, *Phys. Rev. A* **1994**, *50*, 1675.
[59] R. Jin, D. Boggavarapu, M. Sargent, P. Meystre, H. M. Gibbs, G. Khitrova, *Phys. Rev. A* **1994**, *49*, 4038.
[60] S. M. Ulrich, C. Gies, S. Ates, J. Wiersig, S. Reitzenstein, C. Hofmann, A. Löffler, A. Forchel, F. Jahnke, P. Michler, *Phys. Rev. Lett.* **2007**, *98*, 043906.
[61] M. Pollnau, M. Eichhorn, *Prog. Quantum Electron.* **2020**, *72*, 100255.
[62] R. Köhler, A. Tredicucci, F. Beltram, H. E. Beere, E. H. Linfield, A. G. Davies, D. A. Ritchie, R. C. Iotti, F. Rossi, *Nature* **2002**, *417*, 156.
[63] S. Kumar, *IEEE J. Sel. Top. Quantum Electron.* **2011**, *17*, 38.
[64] P. Bienstman, R. Baets, *Opt. Quantum Electron.* **2001**, *33*, 327.
[65] J. B. Khurgin, G. Sun, *Appl. Phys. Lett.* **2011**, *99*, 211106.
[66] C. Walther, G. Scalari, M. I. Amanti, M. Beck, J. Faist, *Science* **2010**, *327*, 1495.
[67] C. Walther, G. Scalari, M. Beck, J. Faist, *Opt. Lett.* **2011**, *36*, 2623.
[68] C. V. Shank, *Rev. Mod. Phys.* **1975**, *47*, 649.
[69] P. Urquhart, *IEE Proc. -J: Optoelectron.* **1988**, *135*, 385.
[70] A. A. Kaminskiĭ, *Crystalline Lasers: Physical Processes and Operating Schemes*, The CRC Press Laser and Optical Science and Technology Series, CRC Press, Boca Raton, FL **1996**, p. 561.
[71] M. J. Kane, G. Braithwaite, M. T. Emeny, D. Lee, T. Martin, D. R. Wright, *Appl. Phys. Lett.* **2000**, *76*, 943.
[72] M. A. Noginov, V. A. Smirnov, I. A. Shcherbakov, *Opt. Quantum Electron.* **1990**, *22*, S61.
[73] S. Wüthrich, W. Lüthy, H. P. Weber, *J. Appl. Phys.* **1990**, *68*, 5467.
[74] A. N. Alpat'ev, A. L. Denisov, E. V. Zharikov, D. A. Zubenko, S. P. Kalitin, M. A. Noginov, Z. S. Saidov, V. A. Smirnov, A. F. Umyskov, I. A. Shcherbakov, *Sov. J. Quantum Electron.* **1990**, *20*, 780.
[75] R. Beck, K. Gürs, *J. Appl. Phys.* **1975**, *46*, 5224.
[76] N. P. Barnes, E. D. Filer, F. L. Naranjo, W. J. Rodriguez, M. R. Kokta, *Opt. Lett.* **1993**, *18*, 708.
[77] N. P. Barnes, R. E. Allen, *IEEE J. Quantum Electron.* **1991**, *27*, 277.
[78] Y. Wang, F. Jobin, S. Duval, V. Fortin, P. Laporta, M. Bernier, G. Galzerano, R. Vallée, *Opt. Lett.* **2019**, *44*, 395.
[79] S.-L. Wang, S. Wang, X.-K. Man, R.-M. Ma, *Nanophotonics* **2020**, *9*, 3403.
[80] G. P. Agrawal, *Fiber-Optic Communication Systems*, 4th ed., Wiley Series in Microwave and Optical Engineering, Wiley, New York **2010**, p. 603.
[81] C. Javerzac-Galy, A. Kumar, R. D. Schilling, N. Piro, S. Khorasani, M. Barbone, I. Goykhman, J. B. Khurgin, A. C. Ferrari, T. J. Kippenberg, *Nano Lett.* **2018**, *18*, 3138.

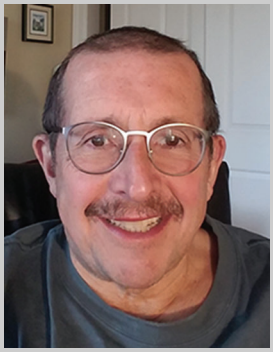

Jacob B. Khurgin graduated with an M.S. in optics from the Institute of Fine Mechanics and Optics in St. Petersburg, Russia in 1979. He received his Ph.D. in electro-physics in 1987 from Polytechnic Institute of NY. In 1988, he joined the ECE department of Johns Hopkins University, where he is a Professor. His research topics include an eclectic mixture of optics of semiconductor nanostructures, nonlinear optical devices, lasers, optical communications, microwave photonics, optomechanics, and condensed matter physics. Currently he is working in the areas of mid-infrared frequency combs, laser refrigeration, plasmonics, silicon photonics, nonreciprocal photonics, nonlinear materials, and others.

Mikhail A. Noginov graduated from Moscow Institute for Physics and Technology (Moscow, Russia) with a Master of Science degree in electronics and automatics, in 1985. In 1990, he received a Ph.D. degree in physical–mathematical sciences from the General Physics Institute of the USSR Academy of Sciences (Moscow, Russia). He is currently a professor of physics at Norfolk State University (USA). His current research interests include plasmonics, metamaterials, and light–matter coupling phenomena. Since 2003, he is a faculty advisor of the OSA student chapter.